European Journal of Medicinal Chemistry 291 (2025) 117583

Contents lists available at ScienceDirect

European Journal of Medicinal Chemistry

journal homepage: www.elsevier.com/locate/ejmech

Research paper

Enabling electrochemical, decarboxylative C(sp^2)–C(sp^3) cross-coupling for parallel medicinal chemistry

Jennifer Morvan [a], Bingqing Tang [a], Pavel Ryabchuk [a], Evelien Renders [a], Stefaan Last [a], Lars Van Eynde [a], Karolina Bartkowiak [a], Peter J.J.A. Buijnsters [a], Alexander X. Jones [a,*], Mary-Ambre Carvalho [a,**], Justin B. Diccianni [b,***]

[a] Global Discovery Chemistry, Janssen Research and Development, Turnhoutseweg 30, Beerse, 2340 Belgium
[b] Global Discovery Chemistry, Janssen Research & Development LLC, 1400 McKean Road, Spring House, PA 19477, United States

A B S T R A C T

Herein we report the development of an automated protocol for coupling aliphatic carboxylic acids and aryl halides under mild, electrochemical conditions. Carboxylic acids are one of the largest pools of commercially available building blocks utilized in parallel medicinal chemistry to expand structure-activity relationships. However, their usage in decarboxylative cross-coupling reactions to forge C(sp^2)–C(sp^3) bonds is low due to challenges associated with direct decarboxylation. Redox-active esters (RAE) are commonly employed to increase the reactivity of carboxylic acids for decarboxylative cross-coupling reactions. Previously, coupling reagent byproducts from in situ generated RAEs proved detrimental to transition metal catalysis. We have developed a purification-free protocol for activating carboxylic acids as *N*-hydroxyphthalimide (NHPI) esters, which are employed in electrochemical decarboxylative cross-coupling in a high-throughput, automated fashion. This automated workflow enables the preparation of compound libraries including PROTACs. By enabling the pool of commercial aliphatic carboxylic acids to be rapidly incorporated into drug-like molecules, this protocol can potentially impact how C(sp^2)–C(sp^3) cross-coupling reactions are performed in drug discovery campaigns.

1. Introduction

Increasing the fraction of sp^3-hybridized C atoms in a molecule can positively impact its properties, such as solubility and permeability, and decrease the likelihood of attrition in drug discovery [1–3]. Incorporation of sp^3-hybridized C atoms can be accomplished through cross-coupling reactions with an appropriate building block. Synthetically, this approach can be challenging compared to cross-coupling two sp^2-hybridized C atoms through reactions such as the Suzuki-Miyaura coupling. Despite significant advances in the field of C(sp^2)–C(sp^3) cross-coupling, uptake in medicinal chemistry has been slow [4–9].

Parallel medicinal chemistry (PMC) enables rapid hit optimization and expansion of structure-activity-relationships (SAR) for a lead compound through iterative design-make-test-analyze (DMTA) cycles [10]. PMC relies on robust methodologies that utilize diverse and widely available building blocks to cover chemical space. Drawing from the pool of aryl and vinyl boronic acids and esters, the Suzuki-Miyaura coupling has proven highly robust for C(sp^2)–C(sp^2) cross-coupling across diverse chemical matter [7]. In the C(sp^2)–C(sp^3) cross-coupling field, several classes of building blocks can be employed under different conditions to effect the desired transformation [11,12]. Since a singular building block class cannot allow access to the entire diversity of commercial C(sp^3) space, methodologies that enable the use of as many monomer classes as possible are important.

Aliphatic carboxylic acids and alcohols comprise two of the largest pools of commercially available C(sp^3) hybridized building block space. Thus, methodologies using these functional groups for C(sp^2)–C(sp^3) cross-coupling are particularly promising for PMC. Notably, there is high degree of orthogonality between the C(sp^3) hybridized chemical space accessible from carboxylic acids *vs.* alcohols (Fig. 1): the overlap between the chemical space of the ~21k products that can be generated from commercial aliphatic carboxylic acids via decarboxylative coupling, and the ~14k products that can be generated from aliphatic alcohols via deoxygenative couplings [13], is only 2.7k compounds. While much work has been done to lower the barrier to running deoxygenative arylation reactions on aliphatic alcohols through the use of automation [14], the barrier to running decarboxylative arylation reactions on commercial carboxylic acids is still high due to the lack of

This article is part of a special issue entitled: Medicinal chemist's toolbox published in European Journal of Medicinal Chemistry.

* Corresponding author.
** Corresponding author.
*** Corresponding author.
E-mail addresses: ajones40@its.jnj.com (A.X. Jones), mcarva11@its.jnj.com (M.-A. Carvalho), jdiccian@its.jnj.com (J.B. Diccianni).

https://doi.org/10.1016/j.ejmech.2025.117583
Received 23 December 2024; Received in revised form 21 February 2025; Accepted 28 March 2025
Available online 2 April 2025

automated protocols, the requirement of strong oxidants to effect direct decarboxylation due to the high redox potentials of carboxylic acids [15], and the necessity of purifying activated esters for use in coupling reactions [16–20].

A recent set of publications by the Baran group details the decarboxylative arylation of redox-active esters (RAE) under electrochemical conditions (Fig. 2A) [21–26]. This methodology offers a mild, base-free avenue to use aliphatic carboxylic acids in C(sp^2)–C(sp^3) cross-coupling reactions. The utility of this method for a PMC group is limited by the requirement of activating the carboxylic acids as the *N*-hydroxyphthalimide (NHPI) esters and individually purifying them. While *in-situ* generated NHPI esters can be employed, the air-tolerance of the method is compromised, and yields suffer [21]. While the chemical space coverage offered by this method is immense, the reaction set up is time-consuming and labor intensive. Additionally, using the IKA ElectraSyn, only six preparative scale reactions can be run in parallel with a required volume of >3 mL/reaction, which is challenging when working on PMC reaction scales (50–100 μmol/0.5–1 mL). While the use of the IKA e-Hive allows 24 reactions to be run in parallel, the inability to run constant current experiments, limited electrode materials, and current density considerations limit its use as a preparative device. Additionally, the non-standard footprint precludes its compatibility with many automated and robotic platforms.

Recognizing the potential of this methodology, we sought to address the challenges with the reaction set up through automation (Fig. 2B). Specifically, we required that our workflow generate chemically diverse C(sp^2)–C(sp^3) coupled products in reproducible yields across a 24-well plate. All reactions should be performed in air, and intermediate NHPI esters should be synthesized and coupled without purification. Parallel electrochemical reactions should be run on typical PMC scales to access compound libraries in sufficient quantities for biological testing after High-Throughput Purification (HTP). We envisioned using solid handling robotics to deliver a solid-supported condensation reagent that could subsequently be filtered off after reaction between carboxylic acids and *N*-hydroxyphthalimide, delivering NHPI esters without the need for chromatographic purification or aqueous workup. At this point, the NHPI esters could be used for a number of decarboxylative transformations under thermal [17,27–29], photoredox [30,31] and/or electrochemical conditions [21–26,32]. Liquid handling robotics could be used to execute the sequence of NHPI dosing, reaction filtration, and addition of the electrochemical reaction components.

Several electrochemical reactors are commercially available for parallel batch [33–37] and flow synthesis [38,39]. Flow library synthesis was not explored in this transformation due to heterogeneity of the reaction mixtures. In batch, issues to overcome include poor reproducibility when transferring methodologies between reactors or reaction scales (e.g. high-throughput experiment (HTE) scale to preparative scale), and inconsistent results across batch parallel reactors due to the lack of electrochemical control of individual wells [38]. We envisaged that automation would improve reproducibility, by ensuring uniform volumes and reagent stoichiometries between wells, while variability in electrode surface and passivation could be mitigated by standardized washing procedures and the inclusion of $AgNO_3$, respectively.

2. Results & discussion

We began our investigation by screening commercially available solid-supported condensation reagents for synthesizing NHPI ester **1a** (Fig. 3A). The yields were determined by quantitative NMR after removal of the solid-supported reagent by filtration and solvent evaporation. It was found that a silica-supported carbodiimide reagent (entry 6) performed optimally, generating the product in high yield and purity, obviating the need for chromatographic purification of the NHPI ester. Different solvents and base additives were investigated in parallel, using HTE (SI Section 1). Conveniently, using THF without any base gave the highest yield of **1a** (75%, 85% NMR purity).

With optimized conditions for the NHPI ester synthesis in hand, we designed and validated an automated "Play-and-Go" protocol in 24-well plate SBS format (Fig. 3B). Silica-supported carbodiimide was dispensed using the Chronect Quantos® solid-handling robot. Subsequent liquid handling steps, such as adding stock solutions of carboxylic acid and NHPI, were carried out using the Tecan EVO. We validated the methodology using both orbital stirring and shaking to mix the identical reactions to assess reproducibility. After reaction completion, suspensions were filtered. Washing with DMF ensured sufficient recovery without excess volumes of solvent. Gratifyingly, we observed an average yield of 63% ± 1.3% across the plate. The dead volume of liquid handling robotic systems accounts for the lower yield compared to individual reactions run manually (75% *vs* 63%). The automation yields were acceptable given that the carboxylic acid is generally used in excess and is the less precious material.

A selection of 24 diverse NHPI esters were successfully synthesized and isolated after a simple filtration (Fig. 3C). Primary (**1b-d**), secondary (**1e-f**), and tertiary (**1g-1h**) NHPI esters could be obtained in good yields, including a bicyclo[1.1.1]pentane carboxylic acid (**1h**). NHPI esters with alpha-heteroatoms are particularly interesting because the stability of other radical precursors, such as alcohols, amines or alkyl halides with alpha-heteroatoms is limited. Carboxylic acids with both nitrogen (**1i-k**) and oxygen (**1l-o**) heteroatoms could be derivatized to the NHPI esters. Amides (**1p**), tertiary amines (**1q**), and BPin groups (**1r**) were tolerated. Benzylic carboxylic acids (**1s-t**) were also competent coupling partners. Acids containing protic amide (**1u**) and Fmoc (**1v**) groups were competent, suggesting possible applications in amino acid derivatization. Excellent functional group tolerance was observed for secondary (**1w**) and tertiary (**1x**) alcohols, which could potentially form ester byproducts.

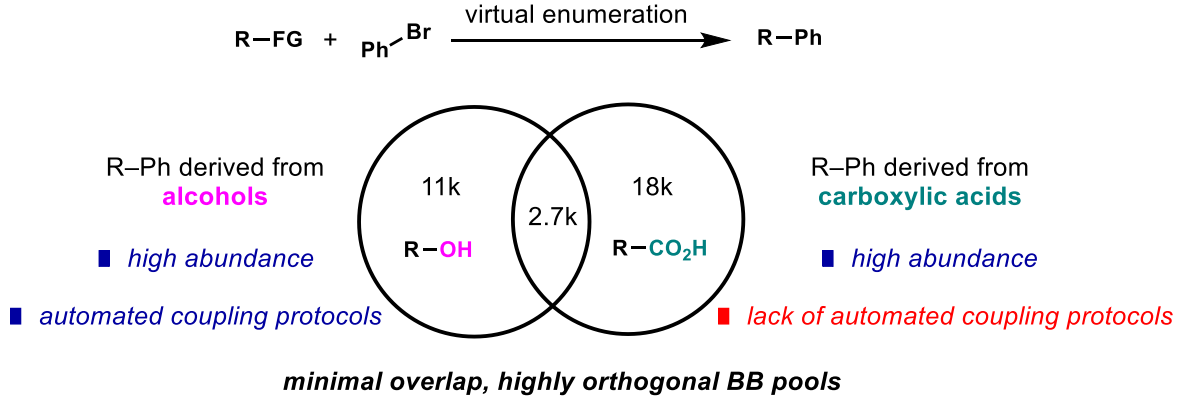

Fig. 1. Building block orthogonality between commercially available alkyl alcohols and carboxylic acids for sp^2-sp^3 cross-coupling.

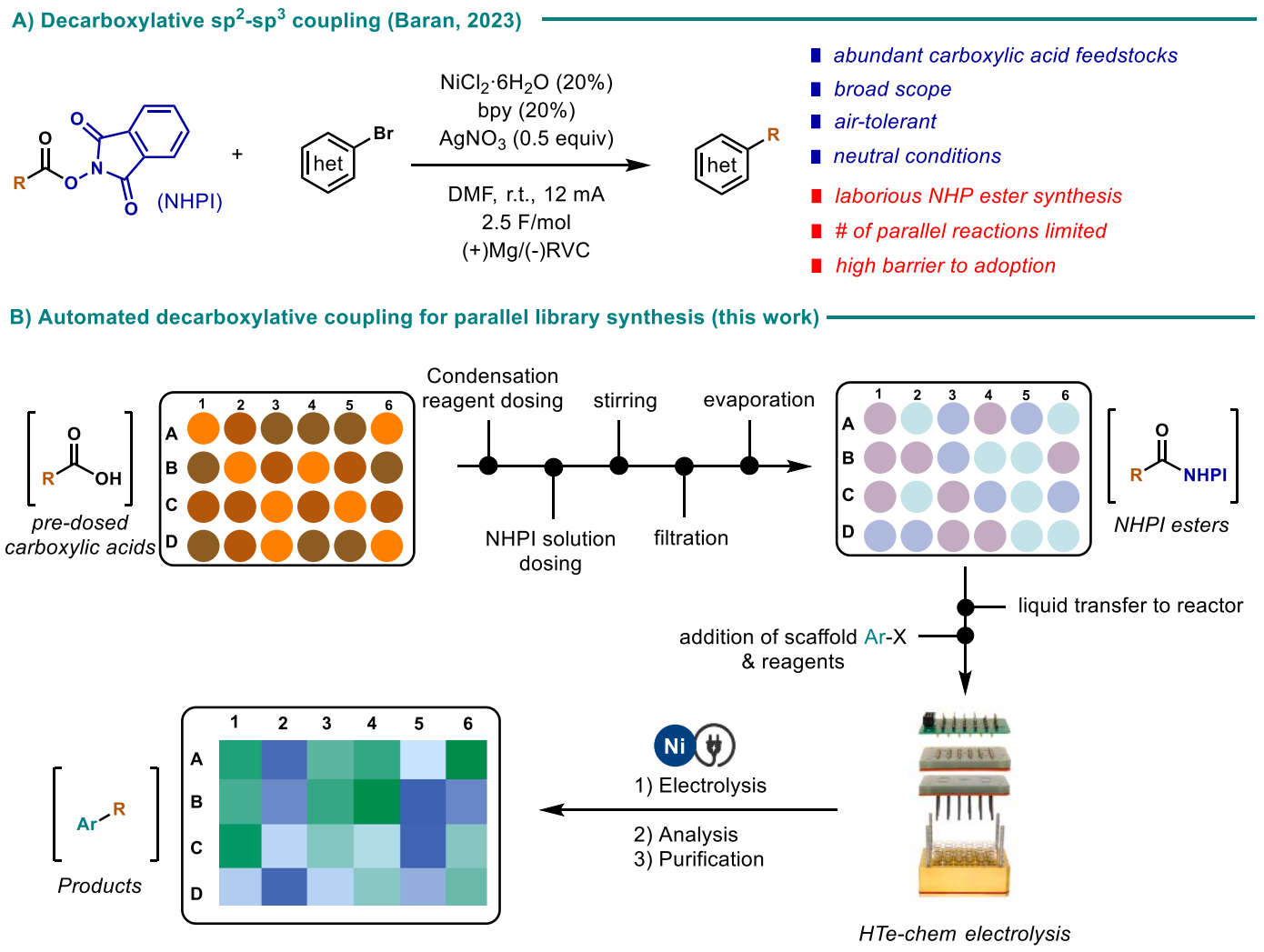

Fig. 2. A) Literature precedent for electrochemical decarboxylative sp^2-sp [3] cross-coupling; B) Desired workflow for automated decarboxylative coupling library synthesis.

Using the automated NHPI ester synthesis workflow, we were now poised to begin optimizing and automating the electrochemical decarboxylation (Fig. 4A). We chose the coupling of 4-tetrahydropyran carboxylic acid **1** and 4-bromophenyl difluoromethyl sulfone **2** as a model reaction on a 50 μmol scale at a reaction concentration of 0.1 M. Aryl halide **2** was selected because the difluoromethyl sulfone moiety is known to be base-sensitive [40] and had previously decomposed under other C(sp^2)–C(sp^3) cross-coupling conditions with basic additives in our hands. The original report employs the IKA ElectraSyn for the cross-coupling reactions. While this device works well for making individual compounds, when running PMC libraries, we are concerned with making small quantities of many compounds to explore SAR with limited material. The need to reduce material consumption per analog synthesized led us to investigate the HTe-chem as an electrochemical device enabling us to synthesize 24 compound libraries in parallel on a small scale. While the HTe-chem enables us to run more reactions in parallel, the choices of electrode material and electrode size are limited. Reticulated vitreous carbon (RVC) electrodes offer high surface area, but this material is fragile and difficult to machine into the small sizes necessary for use in the HTe-chem. We were also aware that replacing RVC with lower surface area electrodes could impact reproducibility due to electrode passivation. Baran et al. [26] describe that $AgNO_3$ additive reduces passivation, providing a possible work-around solution.

Unable to replicate the exact conditions used in the IKA Electrasyn with the HTe-chem, we examined different electrode materials, solvents, and equivalents of $AgNO_3$ to optimize the model reaction (SI section 2). Graphite rods were an acceptable replacement for the RVC electrodes, in combination with 0.5 equiv. $AgNO_3$ (SI section 2.4). DMF gave the highest yield of the screened solvents (SI section 2.1).

Continuous parameters such as current, F/mol, concentration and equivalents of NHPI ester were screened. Optimal results with the model substrate were obtained at 3 mA current (6 mA/cm^2) and 2.8 F/mol (SI section 2.2 - 2.3). Higher current caused more frequent passivation and, with some scaffolds, led to decomposition of the products. Longer reaction times (up to 5.6 F/mol) were detrimental to yield. Reaction volumes between 0.4 and 0.7 mL were essential to balance sufficient electrode immersion and reaction stirring on the tumble stirrer. Concentrations of aryl halide could be increased up to 0.2 M, allowing reactions to be performed on larger scale. Increasing the stoichiometry of NHPI ester beyond two equivalents was detrimental to reactivity (SI section 2.8). Finally, we screened different ligands and Ni sources. Several ligands performed well in the reaction (SI section 2.6), but ultimately, 2,2′-bipyridine and $NiCl_2.6H_2O$ gave the highest yields when using crude NHPI esters generated through the automated workflow (SI section 2.7). Optimal results of 87% LC yield were obtained.

We then sought to validate the automated execution of the entire reaction sequence from carboxylic acid activation to electrochemical coupling (Fig. 4B), to determine the reproducibility of the workflow. After the automated NHPI ester synthesis step was completed, a Tecan EVO liquid handling system was used to transfer solutions of the crude

A) Optimization of NHPI coupling

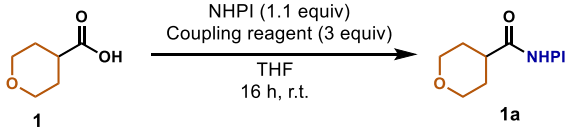

Entry	Supported coupling Reagent	Yield (Purity) (%, NMR)
1	IIDQ-PS (Nova Biochem)	45 (50)
2	N-Bn-N-Cy-carbodiimide – polymer bound (Sigma)	66 (75)
3	EDC – silica bound (SiliCycle)	<1 (<2)
4	EDC – polymer bound (Sigma)	17 (50)
5	Carbodiimide-PS (Biotage, 800370)	64 (95)
6	**Carbodiimide – Silica bound (SiliCycle, R70530B)**	**75 (85)**

B) Automation of NHPI Ester Synthesis

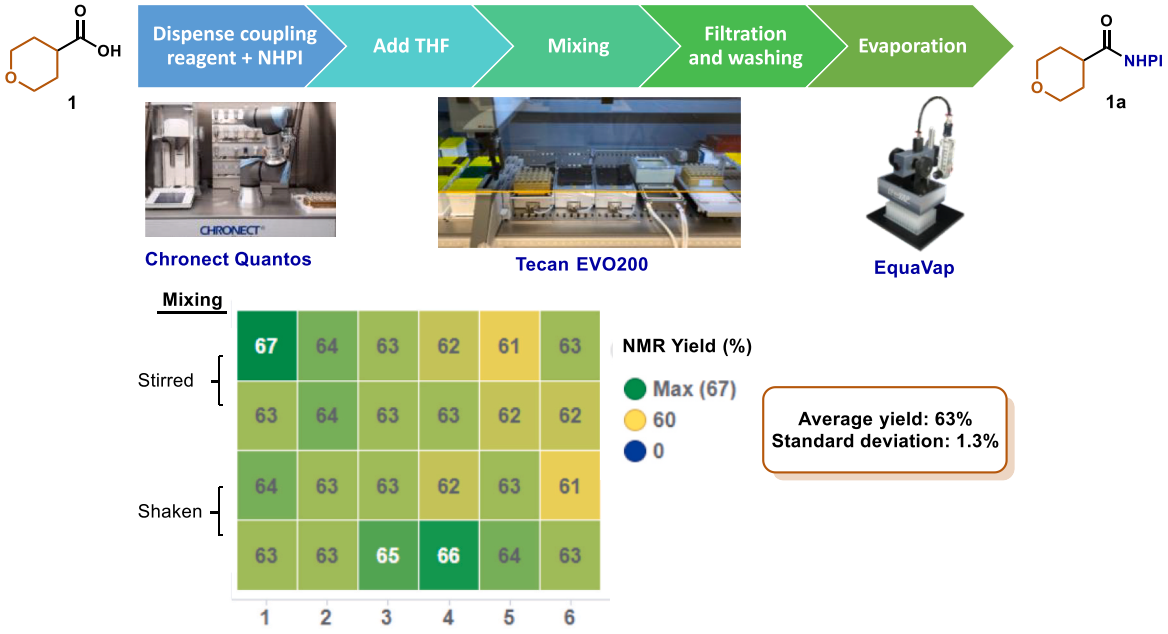

C) Scope of automated NHP ester synthesis protocol

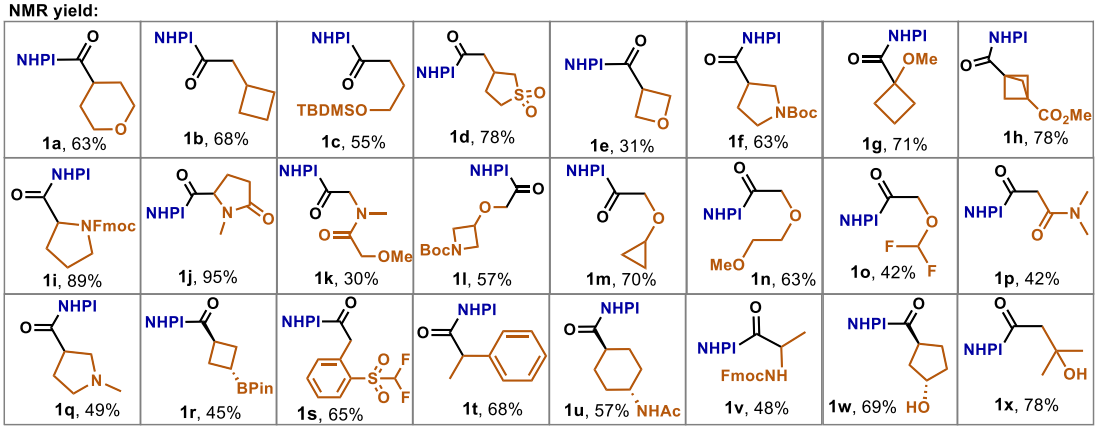

Fig. 3. A) Solid-supported condensation reagent screening for NHPI ester synthesis; B) Automation protocol and results for the parallel synthesis of **1a** with mixing via orbital stirring (top) and shaking (bottom); C) Scope of automated NHPI ester synthesis (yields were determined by quantitative proton NMR with 1,3,5-trimethoxybenzene as internal standard).

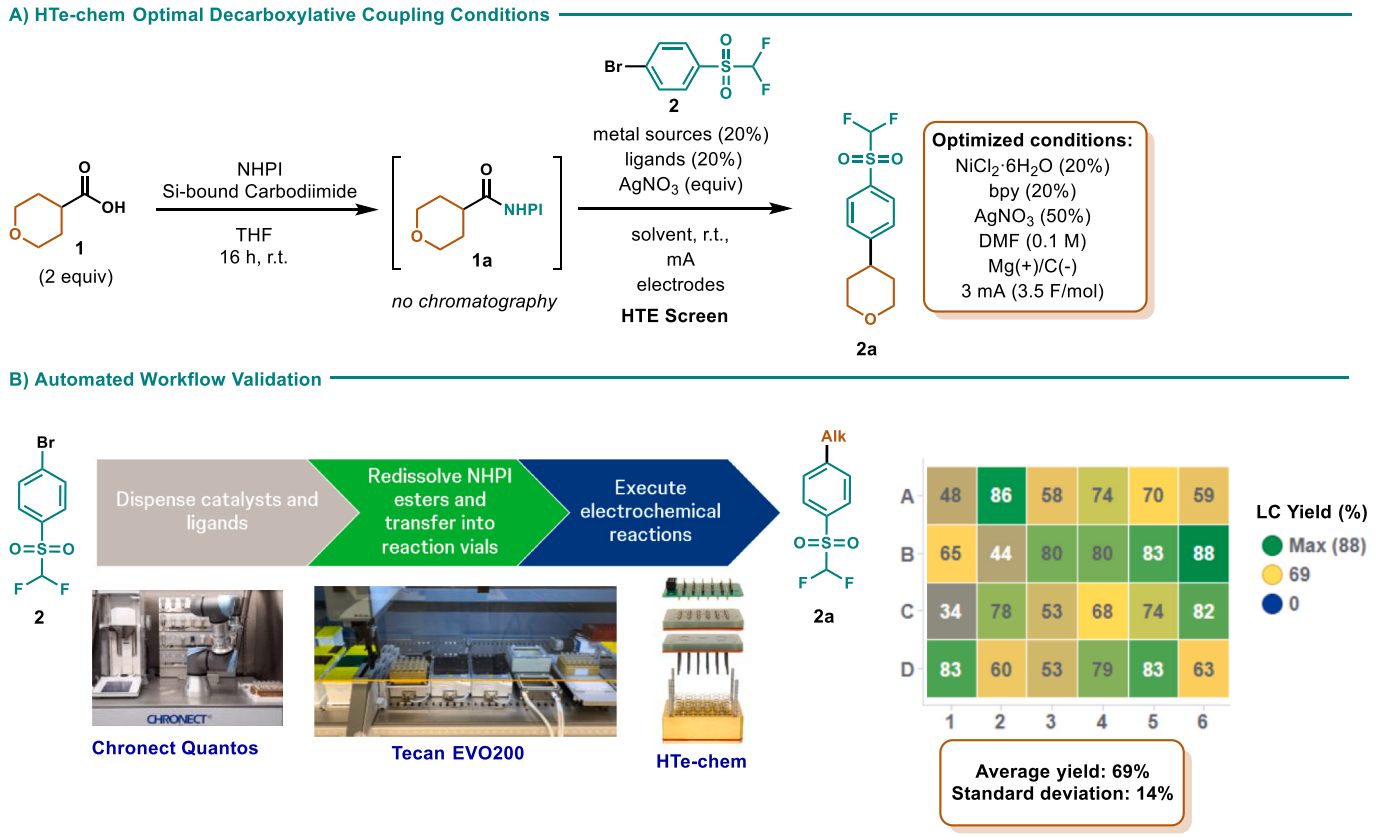

Fig. 4. Reproducibility of automated electrochemical decarboxylative coupling protocol with model substrate (yields were determined by LCMS with a calibration curve with 4-ditertbutylbuphenyl as internal standard).

NHPI ester and add in solutions of the catalytic components of the reaction as well as aryl halide **2** (50 μmol) to a 24-well 1 mL plate (SI section 4). Our fully automated procedure proceeded with an average LC yield of 69% and a standard deviation of 14% over two steps. We attribute the standard deviation to the system's sensitivity to passivation due to graphite's greatly reduced surface area relative to RVC in the original procedure.

Next, we applied the workflow to prepare C(sp^2)–C(sp^3) coupling libraries using two med chem-like scaffolds, **3** and **4**, and 24 different carboxylic acid building blocks. Our goal was to test the workflow with a realistic scenario, where a drug-like aryl halide core was functionalized at a late stage with various carboxylic acid building blocks to explore diversity. Reactions were performed in parallel on an 80 μmol scale (0.15 M), at 1.5 mA until 4 F/mol had been delivered. Two equivalents of carboxylic acids were used for initial NHPI ester synthesis. The results are summarized in Fig. 5A, and both LC yields and isolated yields from HTP are shown. A diverse range of alkyl substituents were accessible. Aryl methylation could be accomplished (**3a**) in 21% isolated yield. Primary carboxylic acids were competent coupling partners (**3b-e**, **4b-d**) including neopentyl acid derivative (**4f**). Secondary carboxylic acids (**3g-j**, **4g**, **4i**) could also be used successfully in this transformation. Pleasingly, quaternary cyclobutane derivatives **3k** and **4k**, and bicyclo [1.1.1]pentane substituted **4l** could be obtained in isolable quantities. We successfully demonstrated the coupling of carboxylic acids with alpha-heteroatoms (**3m-s**, **4m-s**) which generate products inaccessible with most other alkyl radical precursors. The alpha-heteroatom containing acids coupled more effectively with aryl iodide **3** than aryl bromide **4** and overall gave isolated yields between 14 and 24%. Protic functional groups **3u**, **4u** were tolerated, including an Fmoc alanine derivative which generated **3v**. The corresponding analog (**4v**) starting from aryl bromide **4** was not observed. Benzylic carboxylic acids were also employed in the reaction giving product **3w**. In several cases, product was observed by LCMS, but could not be isolated in sufficient quantities or purity for full characterization: including oxetane derivative **3h**, and alpha carbonyl containing carboxylic acid **3t**. Products derived from a carboxylic acid with an alpha difluoromethyl ether (**3s**, **4s**) were not isolated. Coupling a more electron-deficient benzylic carboxylic acid, containing a difluoromethyl sulfone failed to generate **3x** and **4x**. When using aryl bromide **4**, dialkylation byproducts derived from coupling both at the bromide and chloride were observed by LCMS in some cases.

Both the unsubstituted NHPI (R═H) and 2-hydroxy-5-methoxyisoindoline-1,3-dione (R = OMe) OMe–NHPI esters were synthesized from the carboxylic acids using the automated protocol and assessed in the decarboxylative coupling reaction with aryl iodide **3**. The product distributions are shown in Fig. 5B. The OMe–NHPI ester offers slower decarboxylation, which may help match the rate of oxidative addition when the aryl halide is less reactive, or the NHPI ester is prone to rapid decarboxylation [41]. The success rate of the library using aryl iodide **3** was 14/24 with unsubstituted NHPI esters, and 18/24 using OMe–NHPI esters. The average yields across the NHPI-ester and OMe–NHPI ester libraries were 12%, and 18%, respectively. The higher success rate observed using OMe–NHPI esters is due to the minimization of the Ar–Ar coupling side product. Aryl-aryl coupling is formed by off-cycle electrochemical reduction of oxidative addition complexes when the rate of alkyl radical formation is mis-matched [41]. Alpha-heteroatom containing NHPI esters are particularly prone to rapid decarboxylation, and therefore the greatest improvements in yield between NHPI and OMe–NHPI esters are for this class of BB. Other side-products, including phenol formation (Ar-OH) and dehalogenation (Ar–H) showed less dependence on NHPI substitution (Fig. 5B).

After successfully performing the coupling reaction on carboxylic acids containing base-sensitive functional groups, we became interested in applying this methodology on PROTACs (proteolysis targeting

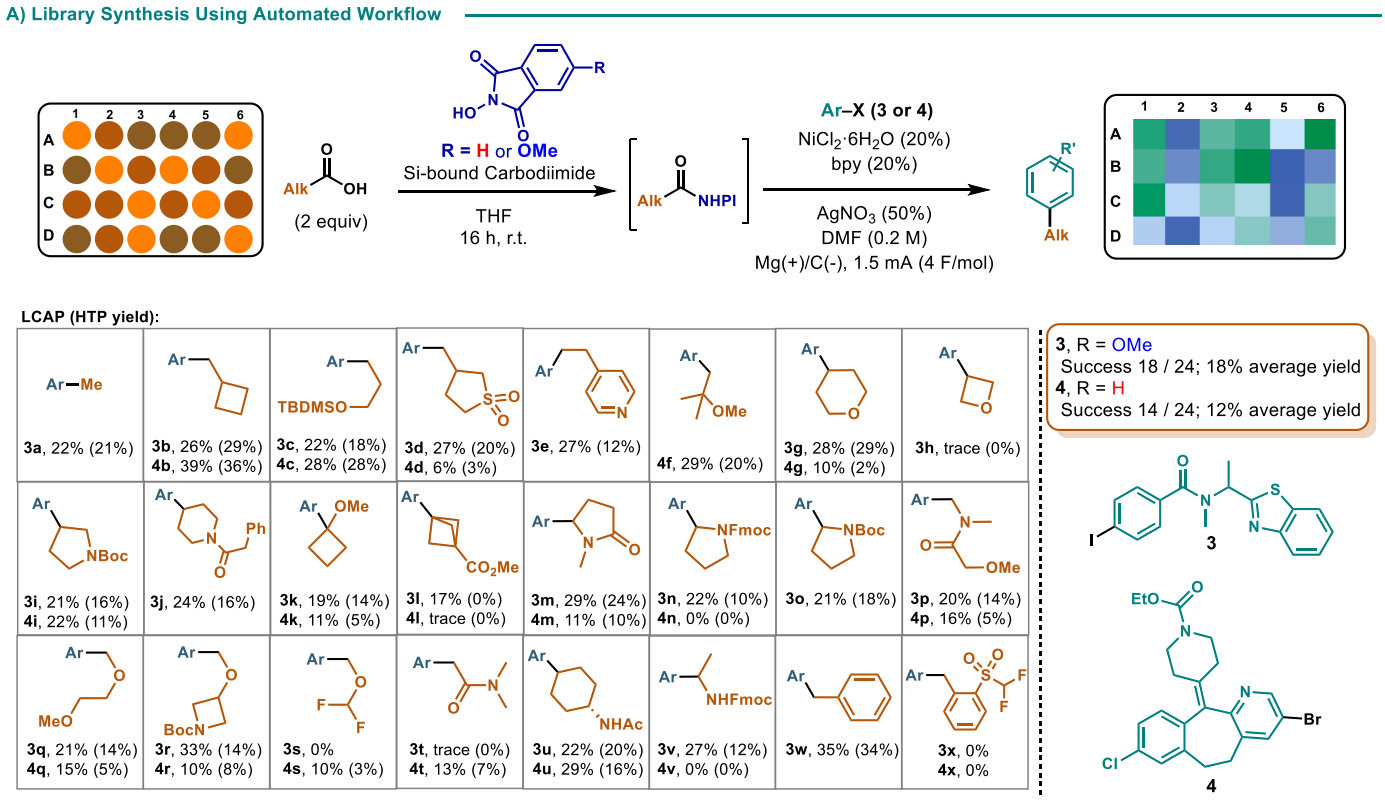

Fig. 5. A) Library synthesis results are reported as LCAP (Liquid Chromatography Area Percentage) values and isolated HTP yields in parentheses; B) distribution of LC product yields across library with aryl iodide **3**, comparing acid activation with OMe–NHPI (blue, left) and H–NHPI (red, right). Ar-Alk refers to products **3a-3x**; Ar–Ar is aryl-aryl homocoupling; Ar-OH is formation of phenol by-product; and Ar–H refers to aryl dehalogenation. (For interpretation of the references to colour in this figure legend, the reader is referred to the Web version of this article.)

chimeras) containing base-sensitive glutarimide moieties. The base-sensitivity of the glutarimide moiety can hamper cross-coupling reactions due to decomposition of the starting materials or products. Our strategy was to activate commercial carboxylic acid-containing partial PROTACs as the NHPI esters and couple these onto the protein of interest (POI) binders to evaluate warhead-linker combinations rapidly. By performing a decarboxylative C(sp^2)–C(sp^3) coupling, instead of the more traditional approach of amidation, the pharmacokinetic and physiochemical properties of the resulting PROTACs can be improved [42]. Furthermore, to the best of our knowledge, this is the first example

of C(sp^2)–C(sp^3) coupling directly on commercially available partial PROTACs. In previous reports, bifunctional linker libraries are step-wise connected to the POI binder before C(sp^2)–C(sp^3) coupling to an aryl-halide containing CRBN-warhead [25].

A set of 24 commercially available CBRN (Cereblon) ligands was assembled with both thalidomide and lenalidomide warheads represented, as well as a range of linker lengths and functional groups to test the methodology on challenging, base-sensitive molecules. Coupling was demonstrated with aryl iodide **3** as a model POI binder (Fig. 6). The automated workflow was essential to minimize the chemist's exposure to these potentially teratogenic compounds. Reaction conditions were the same as for library synthesis above except swapping THF for DMF for the first step of acid activation to better solubilize the partial PROTACs and thus increase recovery of the NHPI esters. For these molecules, NHPI and OMe–NHPI esters gave similar yields of C(sp^2)–C(sp^3) products, but byproducts from the OMe–NHPI esters were responsible for low recoveries due to co-elution during purification. Consequently, LC and isolated yields of the library using NHPI are shown in Fig. 6.

Overall, 20/24 PROTACs could be accessed in isolable quantities, with an average yield of 14%. While the yields are modest, access to the targets is paramount for medicinal chemistry purposes. Hence, a lower yield is often acceptable if the reaction enables enough material to be synthesized for assaying. Primary carboxylic acids with ether (**5a**) and aniline (**5b-c**) linkages were coupled to **3** in 28, 15 & 29% yield, respectively. The length of the linker region significantly affected reaction success: ether **5d** with a 3-carbon linker was observed by LC but could not be isolated. Thioether **5f** and ether **5g** with 2-carbon linkers were not observed. The piperazine linkage in **5e** was incompatible with the reaction conditions. To directly compare the compatibility of thalidomide and lenalidomide motifs with the methodology, compounds **5h** and **5i** were synthesized, respectively, and were found to be compatible with the reaction conditions. Both lenalidomide derivatives **5i**, which has the linker attached at the 7-position, and **5j**, which has the linker attached at the 6-position, had similar reactivity by LC, but **5j** could be isolated in higher yield (26%) by HTP. Lenalidomide derivatives with benzylic carboxylic acids could also be derivatized at multiple positions on the aromatic ring (**5k-l**, **5x**). Secondary carboxylic acids were competent in the arylation (**5m**, **5u-v**). Substrates with heteroatoms alpha to the carboxylic acid were more challenging (**5n-t**, **5w**), but in all cases provided isolable quantities except **5r**.

3. Conclusion

In conclusion, we have developed an automated, parallel workflow to first activate carboxylic acids as their NHPI esters without chromatographic purification, then utilize those NHPI esters in a decarboxylative, electrochemical arylation reaction. The broad scope of the methodology was demonstrated by coupling a diverse set of carboxylic acid targets with drug-like aryl halides. The methodology was extended to the derivatization of carboxylic acid-containing partial PROTACs featuring thalidomide and lenalidomide motifs. Importantly, the automated protocol developed to execute this reaction enhances safety by minimizing exposure to potentially teratogenic compounds. This advance enables the chemical diversity of aliphatic carboxylic acids to be rapidly incorporated into drug-like molecules in an automated, high-throughput fashion. The orthogonal coverage of chemical space that carboxylic acids offer, relative to aliphatic alcohols, and the functional group tolerance of the methodology, as exemplified by the coupling of carboxylic acids with base-sensitive Fmoc groups, difluoromethyl sulfones, and glutarimide motifs, make this an attractive avenue for increasing Fsp^3 in drug discovery campaigns. Future directions include extending this methodology beyond amino acids to peptides as well as performing C(sp^3)–C(sp^3) cross-couplings. Other methodologies where NHPI esters are employed will also be explored. We envision future improvements in parallel electrochemical reactors, such as the ability to control potential and current for individual wells, compatibility with larger reaction vessels, and the ability to vary the electrode surface area, will expand opportunities for further developments in this field.

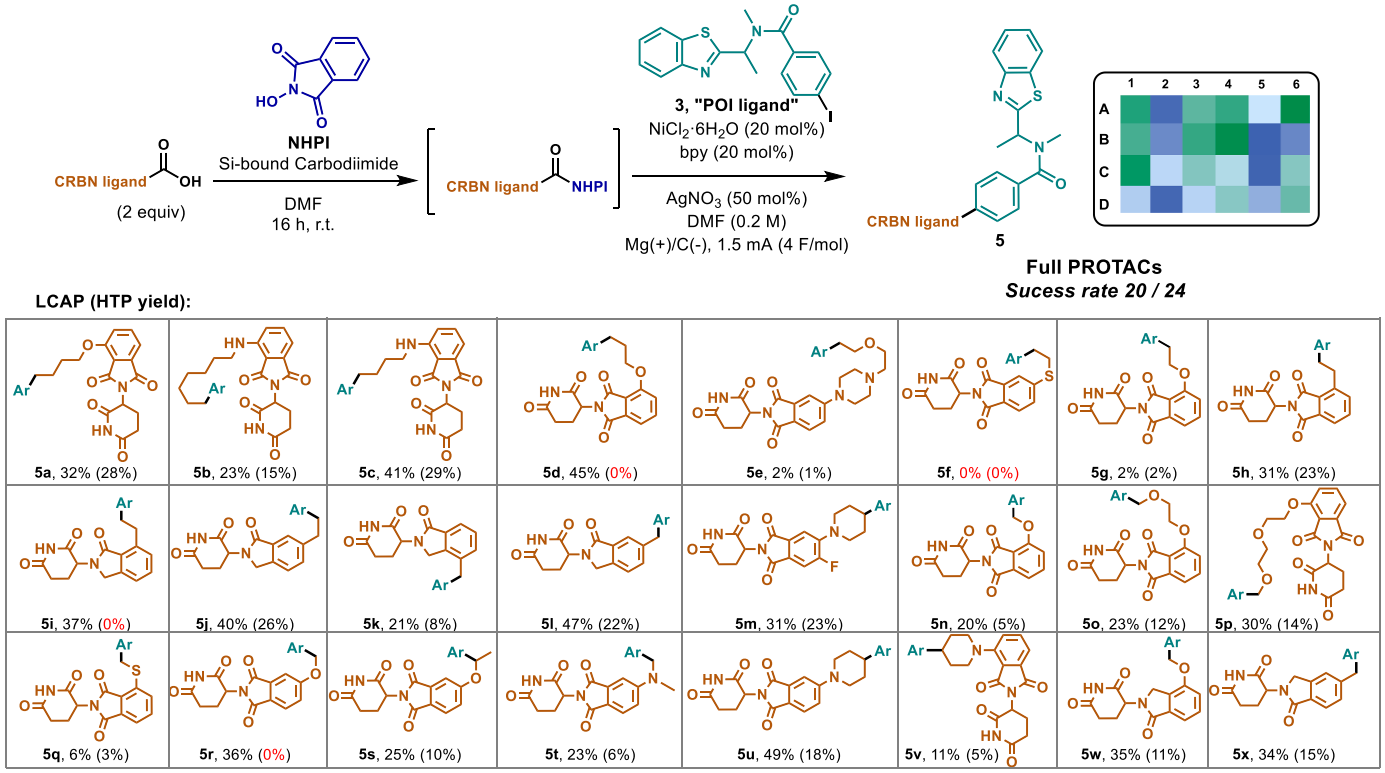

Fig. 6. Protac library synthesis results reported as LCAP (Liquid Chromatography Area Percentage) values and isolated HTP yields in parentheses.

CRediT authorship contribution statement

Jennifer Morvan: Writing – review & editing, Writing – original draft, Methodology, Investigation, Data curation, Conceptualization. **Bingqing Tang:** Methodology, Investigation. **Pavel Ryabchuk:** Writing – review & editing, Methodology, Investigation, Formal analysis. **Evelien Renders:** Methodology, Investigation, Formal analysis. **Stefaan Last:** Writing – review & editing, Methodology, Investigation. **Lars Van Eynde:** Methodology, Investigation. **Karolina Bartkowiak:** Methodology, Investigation. **Peter J.J.A. Buijnsters:** Writing – review & editing, Supervision, Project administration. **Alexander X. Jones:** Writing – review & editing, Writing – original draft, Supervision, Methodology, Formal analysis, Conceptualization. **Mary-Ambre Carvalho:** Writing – review & editing, Writing – original draft, Supervision, Conceptualization. **Justin B. Diccianni:** Writing – review & editing, Writing – original draft, Methodology, Investigation, Conceptualization.

Declaration of competing interest

The authors declare that they have no known competing financial interests or personal relationships that could have appeared to influence the work reported in this paper.

Acknowledgements

J.M. would like to thank V.I.E (Business France) for post-doctoral funding, and B.T. thanks the European Union H2021 research and innovation program under the Marie S. Curie Grant Agreement (MiEL, No.101073003). We thank Jose das Dores Sousa for purification and HRMS data, Alex de Groot for NMR data; Bo Li and Soufyan Jerhaoui for substrate synthesis; and Jesus Alcazar and Zhicai Shi for meaningful discussions.

Appendix A. Supplementary data

Supplementary data to this article can be found online at https://doi.org/10.1016/j.ejmech.2025.117583.

Data availability

All data is described in the supporting information

References

[1] W. Wei, S. Cherukupalli, L. Jing, X. Liu, P. Zhan, Fsp3: a new parameter for drug-likeness, Drug Discov. Today 25 (10) (2020) 1839–1845. https://doi.org/10.1016/j.drudis.2020.07.017.
[2] F. Lovering, J. Bikker, C. Humblet, Escape from flatland: increasing saturation as an approach to improving clinical success, J. Med. Chem. 52 (21) (2009) 6752–6756. https://doi.org/10.1021/jm901241e.
[3] F. Lovering, Escape from Flatland 2: complexity and promiscuity, MedChemComm 4 (3) (2013) 515–519, 10.1039/C2MD20347B, https://doi.org/10.1039/C2MD20347B.
[4] S.D. Roughley, A.M. Jordan, The medicinal chemist's toolbox: an analysis of reactions used in the pursuit of drug candidates, J. Med. Chem. 54 (10) (2011) 3451–3479. https://doi.org/10.1021/jm200187y.
[5] W.P. Walters, J. Green, J.R. Weiss, M.A. Murcko, What do medicinal chemists actually make? A 50-year retrospective, J. Med. Chem. 54 (19) (2011) 6405–6416. https://doi.org/10.1021/jm200504p.
[6] N. Schneider, D.M. Lowe, R.A. Sayle, M.A. Tarselli, G.A. Landrum, Big data from pharmaceutical patents: a computational analysis of medicinal chemists' bread and butter, J. Med. Chem. 59 (9) (2016) 4385–4402. https://doi.org/10.1021/acs.jmedchem.6b00153.
[7] D.G. Brown, J. Boström, Analysis of past and present synthetic methodologies on medicinal chemistry: where have all the new reactions gone? J. Med. Chem. 59 (10) (2016) 4443–4458. https://doi.org/10.1021/acs.jmedchem.5b01409.
[8] J. Boström, D.G. Brown, R.J. Young, G.M. Keserü, Expanding the medicinal chemistry synthetic toolbox, Nat. Rev. Drug Discov. 17 (10) (2018) 709–727. https://doi.org/10.1038/nrd.2018.116.
[9] E. Speckmeier, T.C. Maier, ART—An amino radical transfer strategy for C(sp2)–C(sp3) coupling reactions, enabled by dual photo/nickel catalysis, J. Am. Chem. Soc. 144 (22) (2022) 9997–10005. https://doi.org/10.1021/jacs.2c03220.
[10] A.W. Dombrowski, A.L. Aguirre, A. Shrestha, K.A. Sarris, Y. Wang, The chosen few: parallel library reaction methodologies for drug discovery, J. Org. Chem. 87 (4) (2022) 1880–1897. https://doi.org/10.1021/acs.joc.1c01427.
[11] A.W. Dombrowski, N.J. Gesmundo, A.L. Aguirre, K.A. Sarris, J.M. Young, A. R. Bogdan, M.C. Martin, S. Gedeon, Y. Wang, Expanding the medicinal chemist toolbox: comparing seven C(sp2)–C(sp3) cross-coupling methods by library synthesis, ACS Med. Chem. Lett. 11 (4) (2020) 597–604. https://doi.org/10.1021/acsmedchemlett.0c00093.
[12] Y. Wang, I. Haight, R. Gupta, A. Vasudevan, What is in our kit? An analysis of building blocks used in medicinal chemistry parallel libraries, J. Med. Chem. 64 (23) (2021) 17115–17122. https://doi.org/10.1021/acs.jmedchem.1c01139.
[13] Search Performed on 9/1/24 of the Enamine Database for Compounds Containing Only One of the Desired Functional Groups.
[14] W. Liu, J. Mulhearn, B. Hao, S. Cañellas, S. Last, J.E. Gómez, A. Jones, A. De Vera, K. Kumar, R. Rodríguez, et al., Enabling deoxygenative C(sp2)-C(sp3) cross-coupling for parallel medicinal chemistry, ACS Med. Chem. Lett. 14 (6) (2023) 853–859. https://doi.org/10.1021/acsmedchemlett.3c00118.
[15] R. Xia, M.-S. Xie, H.-Y. Niu, G.-R. Qu, H.-M. Guo, Radical route for the alkylation of purine nucleosides at C6 via minisci reaction, Org. Lett. 16 (2) (2014) 444–447. https://doi.org/10.1021/ol4033336.
[16] G. Laudadio, M.D. Palkowitz, T. El-Hayek Ewing, P.S. Baran, Decarboxylative cross-coupling: a radical tool in medicinal chemistry, ACS Med. Chem. Lett. 13 (9) (2022) 1413–1420. https://doi.org/10.1021/acsmedchemlett.2c00286.
[17] K.M.M. Huihui, J.A. Caputo, Z. Melchor, A.M. Olivares, A.M. Spiewak, K. A. Johnson, T.A. DiBenedetto, S. Kim, L.K.G. Ackerman, D.J. Weix, Decarboxylative cross-electrophile coupling of N-hydroxyphthalimide esters with aryl iodides, J. Am. Chem. Soc. 138 (15) (2016) 5016–5019. https://doi.org/10.1021/jacs.6b01533.
[18] E. Bombonato, V. Fasano, D. Pecorari, L. Fornasari, F. Castagnini, M. Marcaccio, P. Ronchi, Electrochemical synthesis of unnatural amino acids embedding 5- and 6-membered heteroaromatics, ACS Omega 9 (11) (2024) 13081–13085. https://doi.org/10.1021/acsomega.3c09357.
[19] E. Watanabe, Y. Chen, O. May, S.V. Ley, A practical method for continuous production of sp3-rich compounds from (Hetero)Aryl halides and redox-active esters, Chem. Eur J. 26 (1) (2020) 186–191. https://doi.org/10.1002/chem.201905048.
[20] D.T. Flood, S. Asai, X. Zhang, J. Wang, L. Yoon, Z.C. Adams, B.C. Dillingham, B. B. Sanchez, J.C. Vantourout, M.E. Flanagan, et al., Expanding reactivity in DNA-encoded library synthesis via reversible binding of DNA to an inert quaternary ammonium support, J. Am. Chem. Soc. 141 (25) (2019) 9998–10006. https://doi.org/10.1021/jacs.9b03774.
[21] M.D. Palkowitz, G. Laudadio, S. Kolb, J. Choi, M.S. Oderinde, T.E.-H. Ewing, P. N. Bolduc, T. Chen, H. Zhang, P.T.W. Cheng, et al., Overcoming limitations in decarboxylative arylation via Ag–Ni electrocatalysis, J. Am. Chem. Soc. 144 (38) (2022) 17709–17720. https://doi.org/10.1021/jacs.2c08006.
[22] G. Laudadio, P. Neigenfind, Á. Péter, C.Z. Rubel, M.A. Emmanuel, M.S. Oderinde, T.E.-H. Ewing, M.D. Palkowitz, J.L. Sloane, K.W. Gillman, et al., Nickel-electrocatalytic decarboxylative arylation to access quaternary centers, Angew. Chem. Int. Ed. 63 (8) (2024) e202314617. https://doi.org/10.1002/anie.202314617.
[23] J. Sun, H. Endo, M.A. Emmanuel, M.S. Oderinde, Y. Kawamata, P.S. Baran, Simplified modular access to enantiopure 1,2-aminoalcohols via Ni-electrocatalytic decarboxylative arylation, J. Am. Chem. Soc. 146 (9) (2024) 6209–6216. https://doi.org/10.1021/jacs.3c14119.
[24] G. Laudadio, P. Neigenfind, R. Chebolu, V.D. Blasczak, S.J. Maddirala, M. D. Palkowitz, P.N. Bolduc, M.C. Nicastri, R.K. Puthukanoori, B.R. Paraselli, et al., Synthesis of unnatural amino acids via Ni/Ag electrocatalytic cross-coupling, Org. Lett. 26 (11) (2024) 2276–2281. https://doi.org/10.1021/acs.orglett.4c00474.
[25] P. Neigenfind, L. Massaro, Á. Péter, A.P. Degnan, M.A. Emmanuel, M.S. Oderinde, C. He, D. Peters, T. El-Hayek Ewing, Y. Kawamata, et al., Simplifying access to targeted protein degraders via nickel electrocatalytic cross-coupling, Angew. Chem. Int. Ed. 63 (16) (2024) e202319856. https://doi.org/10.1002/anie.202319856.
[26] S.J. Harwood, M.D. Palkowitz, C.N. Gannett, P. Perez, Z. Yao, L. Sun, H.D. Abruña, S.L. Anderson, P.S. Baran, Modular terpene synthesis enabled by mild electrochemical couplings, Science 375 (6582) (2022) 745–752. https://doi.org/10.1126/science.abn1395.
[27] F. Toriyama, J. Cornella, L. Wimmer, T.-G. Chen, D.D. Dixon, G. Creech, P.S. Baran, Redox-active esters in Fe-catalyzed C–C coupling, J. Am. Chem. Soc. 138 (35) (2016) 11132–11135. https://doi.org/10.1021/jacs.6b07172.
[28] J. Wang, T. Qin, T.-G. Chen, L. Wimmer, J.T. Edwards, J. Cornella, B. Vokits, S. A. Shaw, P.S. Baran, Nickel-catalyzed cross-coupling of redox-active esters with boronic acids, Angew. Chem. Int. Ed. 55 (33) (2016) 9676–9679. https://doi.org/10.1002/anie.201605463.
[29] F. Sandfort, M.J. O'Neill, J. Cornella, L. Wimmer, P.S. Baran, Alkyl−(Hetero)Aryl bond formation via decarboxylative cross-coupling: a systematic analysis, Angew. Chem. Int. Ed. 56 (12) (2017) 3319–3323. https://doi.org/10.1002/anie.201612314.
[30] L.M. Kammer, S.O. Badir, R.-M. Hu, G.A. Molander, Photoactive electron donor–acceptor complex platform for Ni-mediated C(sp3)–C(sp2) bond formation, Chem. Sci. 12 (15) (2021) 5450–5457, 10.1039/D1SC00943E, https://doi.org/10.1039/D1SC00943E.
[31] V.C. Polites, S.O. Badir, S. Keess, A. Jolit, G.A. Molander, Nickel-catalyzed decarboxylative cross-coupling of bicyclo[1.1.1]pentyl radicals enabled by electron donor–acceptor complex photoactivation, Org. Lett. 23 (12) (2021) 4828–4833. https://doi.org/10.1021/acs.orglett.1c01558.

[32] H. Li, C.P. Breen, H. Seo, T.F. Jamison, Y.-Q. Fang, M.M. Bio, Ni-catalyzed electrochemical decarboxylative C–C couplings in batch and continuous flow, Org. Lett. 20 (5) (2018) 1338–1341. https://doi.org/10.1021/acs.orglett.8b00070.

[33] J. Rein, S. Lin, D. Kalyani, D. Lehnherr, High-throughput experimentation for electrochemistry. In *the Power of high-throughput experimentation: general Topics and enabling Technologies for Synthesis and catalysis (volume 1)*, ACS (Am. Chem. Soc.) Symp. Ser. 1419 (2022) 167–187. American Chemical Society.

[34] J. Rein, J.R. Annand, M.K. Wismer, J. Fu, J.C. Siu, A. Klapars, N.A. Strotman, D. Kalyani, D. Lehnherr, S. Lin, Unlocking the potential of high-throughput experimentation for electrochemistry with a standardized microscale reactor, ACS Cent. Sci. 7 (8) (2021) 1347–1355. https://doi.org/10.1021/acscentsci.1c00328.

[35] C. Bottecchia, D. Lehnherr, F. Lévesque, M. Reibarkh, Y. Ji, V.L. Rodrigues, H. Wang, Y.-h. Lam, T.P. Vickery, B.M. Armstrong, et al., Kilo-scale electrochemical oxidation of a thioether to a sulfone: a workflow for scaling up electrosynthesis, Org. Process Res. Dev. 26 (8) (2022) 2423–2437. https://doi.org/10.1021/acs.oprd.2c00111.

[36] L.F.T. Novaes, J. Liu, Y. Shen, L. Lu, J.M. Meinhardt, S. Lin, Electrocatalysis as an enabling technology for organic synthesis, Chem. Soc. Rev. 50 (14) (2021) 7941–8002, 10.1039/D1CS00223F, https://doi.org/10.1039/D1CS00223F.

[37] L.F.T. Novaes, J.S.K. Ho, K. Mao, K. Liu, M. Tanwar, M. Neurock, E. Villemure, J. A. Terrett, S. Lin, Exploring electrochemical C(sp3)–H oxidation for the late-stage methylation of complex molecules, J. Am. Chem. Soc. 144 (3) (2022) 1187–1197. https://doi.org/10.1021/jacs.1c09412.

[38] Morvan, J.; Kuijpers, K. P. L.; Fanfair, D.; Tang, B.; Bartkowiak, K.; van Eynde, L.; Renders, E.; Alcazar, J.; Buijnsters, P. J. J. A.; Carvalho, M.-A.; et al. Electrochemical C−O and C−N Arylation using Alternating Polarity in flow for Compound Libraries. Angewandte Chemie International Edition n/a (n/a), e202413383. DOI: https://doi.org/10.1002/anie.202413383.

[39] Rial-Rodríguez, E.; Williams, J. D.; Cantillo, D.; Fuchß, T.; Sommer, A.; Eggenweiler, H.-M.; Kappe, C. O.; Laudadio, G. An Automated Electrochemical Flow Platform to Accelerate Library Synthesis and Reaction Optimization. Angewandte Chemie International Edition n/a (n/a), e202412045. DOI: https://doi.org/10.1002/anie.202412045.

[40] J.B.I. Sap, C.F. Meyer, J. Ford, N.J.W. Straathof, A.B. Dürr, M.J. Lelos, S.J. Paisey, T.A. Mollner, S.M. Hell, A.A. Trabanco, et al., [18F]Difluorocarbene for positron emission tomography, Nature 606 (7912) (2022) 102–108. https://doi.org/10.1038/s41586-022-04669-2.

[41] D.C. Salgueiro, B.K. Chi, I.A. Guzei, P. García-Reynaga, D.J. Weix, Control of redox-active ester reactivity enables a general cross-electrophile approach to access arylated strained rings, Angew. Chem. Int. Ed. 61 (33) (2022) e202205673. https://doi.org/10.1002/anie.202205673.

[42] C.M. Arndt, J. Bitai, J. Brunner, T. Opatz, P. Martinelli, A. Gollner, K.R. Sokol, M. Krumb, One-pot synthesis of cereblon proteolysis targeting chimeras via photoinduced C(sp2)–C(sp3) cross coupling and amide formation for proteolysis targeting chimera library synthesis, J. Med. Chem. 66 (24) (2023) 16939–16952. https://doi.org/10.1021/acs.jmedchem.3c01613.